JOURNAL OF AIRCRAFT
Vol. 39, No. 1, January–February 2002

Determination of Structural Modes of Vibration Using Digital Photogrammetry

T. G. Ryall*
Aeronautical and Maritime Research Laboratory, Melbourne, Victoria 3001, Australia
and
C. S. Fraser†
University of Melbourne, Melbourne, Victoria 3010, Australia

It is shown that it is possible to recover the three-dimensional modes of vibration of an oscillating structure through an offline digital photogrammetric approach employing only a single video camera. In addition to the camera, the technique requires a high powered synchronized strobe unit and the careful control of fixed sequential delays between the excitation force, the strobe illumination, and the multiple sequence of camera exposures. The dynamic three-dimensional object point triangulation problem is then reduced to a set of static problems by capturing object shape in a number of different phases at a given number of measurement epochs. For each repeatable oscillation cycle, the vibrating object is imaged from a different camera position. The *XYZ* object coordinates of the target array at each sampling epoch can, thus, be determined by photogrammetric triangulation using all images corresponding to the same instant of time within the oscillation cycle. The dynamic mode shape is then determined from the triangulated object points at the various phases. The process is illustrated for the determination of modes of vibration for an aircraft wing section. Note that the advantages of using only a single camera are multifold; the system is cheaper, the system is simpler and, thus, more robust in that multiple cameras do not have to be synchronized, and finally the system has the potential to deliver greater accuracy without having an excessively large number of cameras.

I. Introduction

A FUNDAMENTAL operation in structural dynamics is the determination, either experimentally or theoretically, of both mode shapes and their corresponding frequencies. These modes, of which there are an infinite number, can be shown to be orthogonal to one another when weighted by the mass density. The modes essentially summarize both the inertial and elastic behavior of the structure and as a result form a complete set of functions, a finite number of which can efficiently represent the low-frequency motion of the structure in question.[1,2] A modal expansion is also quite commonly referred to in control systems literature for multi-input multi-output systems and is normally expressed as a state-space model.[3] Experimental determination of mode shapes is of fundamental importance for the analysis of structural dynamics in the aircraft industry, where they are used to check on the validity of, or to improve, finite element models.[4] These models are in turn used to determine the all-important aircraft flutter (stability) boundaries.

The present methods of measuring mode shapes typically require either a single accelerometer, which is moved from point to point, or alternatively a large number of accelerometers, which are placed all over the aircraft. The former method is cheap but time consuming, whereas the latter is much faster, due to parallel processing, but also significantly more expensive. The method employing multiple accelerometers also suffers from the disadvantage of added mass due to the presence of instrumentation and wiring. A prospective alternative to accelerometer-based approaches, which has been adopted for the reported project, is vision-based optical three-dimensional coordinate measurement via digital close-range photogrammetry. This technique, which is also termed vision metrology or videogrammetry, offers a practical, inexpensive, non-interfering method of measuring modes.

Received 29 November 2000; revision received 26 July 2001; accepted for publication 31 July 2001.

*Principal Research Scientist, Airframes and Engines Division, P.O. Box 4331.
†Professor, Department of Geomatics.

II. Offline and Online Vision Metrology

Before discussing the novel application of vision metrology for the measurement of mode shapes, it is useful to offer a brief explanation of the basic principles of this technique. Figure 1 shows a so-called monoscopic/convergent close-range photogrammetric network in which a targeted object is imaged from four different camera station positions. The term convergent describes the nature of the orientation of the camera optical axes for the four image stations. This is distinct from stereophotogrammetry, where the optical axes are constrained to be near parallel to allow human stereo viewing. Through a spatial intersection process, the *XYZ* coordinates of signalized points on the object are determined from both measured *xy* frame coordinates for the corresponding image points and from knowledge of the exterior orientation (three-dimensional position and spatial orientation) of each image. The basic mathematical model for this transformation is given by the well-known collinearity equations,[5,6] namely,

$$x - x_0 + \Delta x = -c(X'/Z')$$
$$y - y_0 + \Delta y = -c(Y'/Z') \tag{1}$$

where

$$\begin{pmatrix} X' \\ Y' \\ Z' \end{pmatrix} = \boldsymbol{R} \begin{pmatrix} X - X^0 \\ Y - Y^0 \\ Z - Z^0 \end{pmatrix}$$

where X', Y', and Z' represent a rotated object space coordinate system with its origin at the camera perspective center and its axes aligned to those of the image coordinate system *xyz*. The collinearity equations describe the perspective transformation between the object space (object point X, Y, Z and perspective center X^0, Y^0, Z^0 with rotation matrix $\boldsymbol{R}$) and image space (image point x, y) for an image recorded with a camera focal length c. Equation (1) also

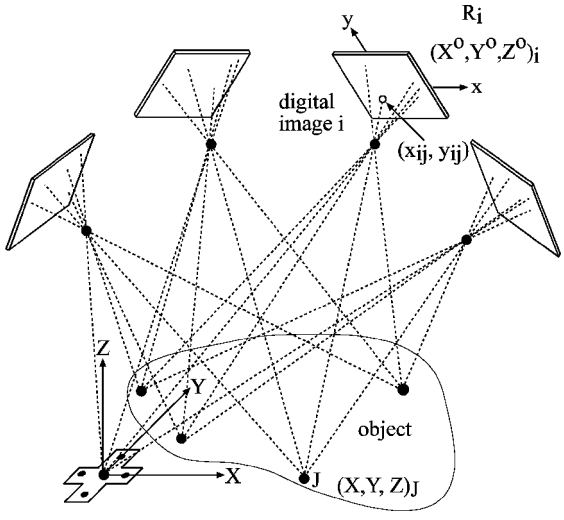

Fig. 1 Convergent close-range photogrammetric network comprising four camera stations.

comprises sensor system calibration terms, namely, the so-called interior orientation or intrinsic parameters, x_0, y_0, and c, and the image coordinate perturbation terms Δx and Δy, which account for the departures from collinearity due mainly to lens distortion. Any photogrammetric network comprising two or more camera stations and more than five object points common to each image constitutes an overdetermined nonlinear observation equation system, the parameters for which can be obtained via a least-squares estimation process. Specifically, on linearization Eqs. (1) can be written as

$$\boldsymbol{v} = \boldsymbol{A}_1\boldsymbol{x}_1 + \boldsymbol{A}_2\boldsymbol{x}_2 + \boldsymbol{A}_3\boldsymbol{x}_3 + \boldsymbol{w} \tag{2}$$

where $\boldsymbol{x}_1$ are the parameters of camera position and orientation, $\boldsymbol{x}_2$ the object point coordinates, and $\boldsymbol{x}_3$ the camera calibration parameters. The $\boldsymbol{A}_i$ matrices are the corresponding configuration matrices, $\boldsymbol{w}$ is the image coordinate discrepancy vector, and $\boldsymbol{v}$ is the vector of residuals of the observed image coordinates. The least-squares solution process for Eqs. (2), which minimizes the quadratic form $\boldsymbol{v}^T\boldsymbol{v}$, is termed the bundle adjustment.[5,6] Although it is possible to solve simultaneously for all parameters $\boldsymbol{x}_i$ within a single multistation convergent imaging network, special attention must be paid to network geometry if a sensor self-calibration is also to be achieved. For the present discussion, we will disregard this aspect and concentrate solely on the recovery of the object point coordinates $\boldsymbol{x}_2$ and sensor exterior orientation $\boldsymbol{x}_1$. Within vision metrology, there are two distinct approaches that can be followed, namely, offline and online (real-time) configurations. In the case of an offline network, the images indicated in Fig. 1 would generally be recorded sequentially with a single camera. After acquisition of all images, of which there may be 3, 10, or even 100, image coordinates are observed, and the solution for the parameters $\boldsymbol{x}_1$ and $\boldsymbol{x}_2$ is obtained via least-squares normal equations formed from Eqs. (2). This means that in addition to the object coordinates X_j, Y_j, and Z_j for each target j, the exterior orientation parameters (X^0, Y^0, and Z^0 with the three angles forming the rotation matrix R) for all camera stations are simultaneously recovered even though they are not explicitly sought within the measuring process. Offline vision metrology is widely used for high-precision measurement with the sectors of large-scale manufacturing and engineering.[7] Innovations such as orientation devices and coded targets, along with intelligent charge-coupled device (CCD) cameras, can be incorporated to enable the off line measurement process to be conducted fully automatically.[8,9] The automated process can be briefly summarized as follows. Let us first imagine that the targeted cross in Fig. 1 comprises four points of known *XYZ* coordinates (i.e., known relative to one another in an arbitrary local Cartesian reference system), which are automatically identifiable within each digital image. After the automatic measurement of all image point coordinates x, y, an initial solution for sensor exterior orientation can be obtained on an image-by-image basis via a spatial resection from the known coordinates of the orientation device:

$$\boldsymbol{v} = \boldsymbol{A}_{1i}\boldsymbol{x}_{1i} + \boldsymbol{w}_i \tag{3}$$

A least-squares approach is again typically adopted for the solution of the six parameters forming $\boldsymbol{x}_{1i}$. Once the preliminary exterior orientation is established, approximate object point coordinates can be computed, again sequentially for each point j, through a series of space intersections in three unknowns. The observation equations follow from Eq. (2) as

$$\boldsymbol{v} = \boldsymbol{A}_{2j}\boldsymbol{x}_{2j} + \boldsymbol{w}_j \tag{4}$$

The offline approach to digital close-range photogrammetry is well documented in the literature because it represents the traditional approach to the restitution of convergent photogrammetric imaging configurations. A general prerequisite for the process is that the shape of the object is invariant throughout the period when the imagery is recorded. The object may of course move during the recording period, but there can be no shape deformation of the target point field. At first sight, then, it would seem that a single-sensor, offline vision metrology approach could not be used to determine the modes of vibration of a shape-variant, oscillating structure.

The second approach to vision metrology, through use of an online (real-time) system configuration, utilizes multiple cameras, which synchronously record the necessary imagery. Thus, in a real-time system, the camera stations in Fig. 1 would each be occupied by a different camera. This configuration is much better suited to dynamic events because the object is recorded at each measurement epoch in an instant of time. The data processing can follow the same sequence as in the offline approach, namely, exterior orientation followed by spatial intersection and then bundle adjustment, though it is quite common to perform a precise initial exterior orientation followed at each measuring epoch by an intersection alone [Eq. (4)].

Thus, if it is desired to track the motion of the object in Fig. 1, a bundle adjustment can first be carried out to achieve an optimal exterior orientation. The camera station parameters are then held fixed, reflecting the stable nature of the multicamera configuration, and at each subsequent recording epoch, the new positions of object points are determined by triangulation, always within a common *XYZ* reference system. Online vision metrology systems are also widely employed in industrial measurement, with the object being tracked usually comprising a targeted touch probe.[9] This gives rise to an optically based real-time three-dimensional coordinate measurement system. The technique of multicamera, online digital photogrammetry has recently been employed by NASA to study vibrations of the large solar arrays on the Hubble Space Telescope.[10] Stereophotogrammetry (using two cameras) has also been tried to study vibrations of aircraft models in wind tunnels.[11]

Based on this cursory introduction alone, one could well surmise that the multicamera, online mode of operation would be logical for the task of monitoring a vibrating structure. Yet, one of the distinctive features of the reported investigation is that an offline, single-sensor vision metrology approach was successfully employed to determine spatial position information on a shape-variant vibrating structure.

III. Offline Measurement of the Shape-Variant Wing

Shown in Fig. 2 is a targeted wing section in a supporting frame, the wing being subjected to vibration forces. It is desired to measure the array of surface points at various instances within the cycle of oscillation. As mentioned earlier, this would logically be approached using an online, multisensor vision metrology approach. To employ single-sensor, offline measurement, the dynamic problem must be reduced to a series of static single-sensor, multistation measurement networks. To achieve this aim, a number of prerequisites must be met.

1) The motion of the oscillating body must be completely reproducible.

2) The motion must be phased locked to a driving reference signal.

3) The recording epochs for the imagery must also be phased locked to that same reference signal.

With these conditions fulfilled, it could be assumed that the shape of the object, the deformed wing section in this case, would be the same at a given instant of time within the repeatable cycle of oscillation, which is induced via a controlled electromagnetic shaker.

A modified version of the Australis software suite for offline digital close-range photogrammetry[12] was to be employed for the image mensuration and photogrammetric data processing phase of the project. In its standard operational mode, Australis performs the automated measurement of each of the images forming the imaging network (Fig. 1). Figure 3 shows a series of labeled targets, both wing section targets subject to vibration, and a small number (single- and double-digit labels) of stable reference points. Once the *xy* image coordinates of each image forming the network for a given epoch are recorded, the spatial intersection to yield *XYZ* object target coordinates can be performed, again within the Australis system.

For the measurement of modes of vibration of the wing section, a variation to this computational procedure was employed. Given that a sequence of 20 or more images was taken from a single camera station position before the camera was moved to the next station and that the shake/vibration sequence was repeated, it was deemed more practical to measure all images from each camera station sequentially. The maximum amplitude of vibration was 2 mm, and, thus, at a imaging scale of approximately 1:100, the position of each target within successive images was repeatable to within about 5 pixels. This meant that following semi-automatic measurement of the first image of a sequence, which could be at the rest position, all remaining *xy* coordinates could be measured with only a minimum of operator intervention. At a given recording epoch, the stable points would retain their labels, but the moving targets would be assigned labels where the first digit defined the frequency of oscillation, the second digit defined the delay or phase, and the last three digits formed the constant location identifier.

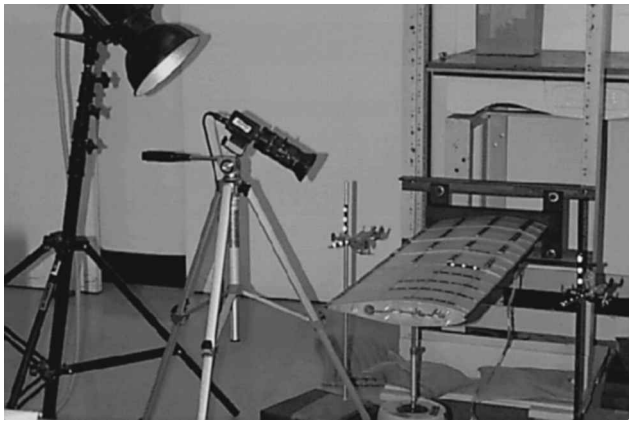

Fig. 2 Imaging configuration for the targeted, vibrating wing section; eight such camera positions employed.

This highly automated image measurement operation allowed the very rapid measurement of the tens of images forming the repeated eight-station triangulation networks. Moreover, the process provided a means to ensure that any instability in the camera exterior orientation could be compensated. A first stage of the computation process was to perform an 32-image triangulation for each frequency. A second and final stage was to compute a bundle adjustment, which facilitated a simultaneous exterior orientation and triangulation for all $8i$ images and $(110i + 12)$ object points, where i is the number of frequencies multiplied by the number of delays. For the nominal $i = 8$, the final bundle adjustment comprised 384 exterior orientation parameters and about 900 object point coordinate parameters.

An important byproduct of the spatial intersections, and especially the final bundle adjustment, is covariance information related to the *XYZ* target point coordinates. The resulting standard errors of triangulation for points on the wing surface were close to 0.05 mm, which was consistent with design expectations. For a vibration test using 64 images, the total image measurement and triangulation phase consumed only a few minutes. Within the repeatable cycles of oscillation, it was desired to capture positional information at 97 targeted wing locations and at 4 phases of motion. The video imagery recorded at each station covered several cycles of oscillation, and optimal images for measurement were chosen on the basis of target illumination. The time delay between the camera exposure and strobe illumination was varied to optimize the contrast between targets and background. An ideal intensity distribution was one which was bimodal, as indicated in Fig. 4, where the spike at a grayscale value of 255 represents the return from the retroreflective targets.

Fig. 3 Object point array of retroreflective photogrammetric targets on the wing section and offwing stable targets.

IV. Image Recording

The video camera used for the project was a Sony CCD camera XC-75CE with an imaging array of 752 (horizontal) × 582 (vertical) pixels. This camera was operated in what is referred to as mode 2 (a stop–restart mode), which allowed control over both the exposure (shutter) time and the epoch at which the frame was grabbed. The exposure time used was 1/10,000th s. Faster exposure times are possible with an external signal, but this shutter speed was considered adequate because the maximum frequency of excitation examined was 17 Hz, which corresponded to a maximum phase error of 0.6 deg. Because of idiosyncrasies of the camera in the start–stop mode, only the second frame contained useful information, the first field of the second frame being recorded after an additional delay of 12.5 ms. This additional delay was on top of any desired delay. The source of illumination used was a high powered flash, which dissipated 6 kJ in 20 ms. This guaranteed that good contrast was possible even for such short exposure times.

In the actual image analysis, video fields rather than frames were employed (because the fields are taken at different times and separated by $\frac{1}{50}$th s), which meant that vertical resolution (number of image rows) was effectively half that of the horizontal (number of columns). A preliminary investigation indicated that the use of video fields alone would have only a minor impact on the precision of measuring target centroids within the imagery. However, because it was known a priori that the error in the y coordinate would likely be twice that in x, the optimal way of treating the data would have been through use of a weighted least-squares approach, where the x-coordinate observations (horizontal) would be assigned twice the weight of those in y (vertical). This would yield parameter estimates that were asymptotically unbiased and that would additionally be minimum variance estimators asymptotically. Although such a weighting scheme could have been accommodated in Australis, indications were that any influence of this basic difference in observational precision between x and y observations would be minimized by ensuring that the camera was rotated through 90 deg for every camera position.

An important issue regarding metric quality, which underpinned the whole method, was that the shaker would produce perfectly repeatable oscillation cycles. This was tested by recording multiple images at different times, when the deformed wing was nominally in the same state. The image coordinates where then measured in each image and were found to be repeatable to within 0.05 pixels. The assumption of shape invariance for a given epoch had, therefore, been experimentally verified.

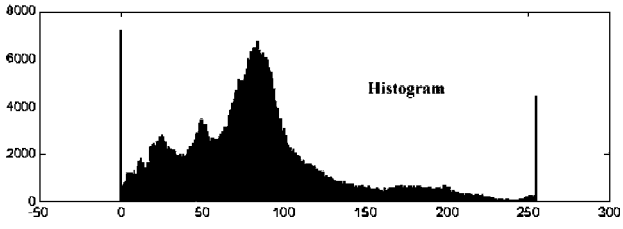

Fig. 4 Histogram of intensity corresponding to image in Fig. 3.

V. Initial Validation of the Method

An initial test was carried out to validate the offline, single-sensor vision metrology approach for measuring the vibrating wing section. This involved a small metal plate with six attached targets being rigidly attached to a shaker, as shown in Fig. 5. As a result, all motion induced by the shaker was purely translational in the vertical direction. Moreover, all moving targets would be displaced by the same amount, and because the shaker is a linear device, a reduction by a fixed amount in its driving voltage should reduce the motion by the same amount. All other targets indicated in Fig. 5 were stationary so as provide a fixed *XYZ* reference coordinate system.

Table 1 shows the peak-to-peak displacements during a cycle of oscillation experienced by the targets labeled 1 and 2, as measured

Table 1 Absolute and relative displacements of points 1 and 2 within the validation test measurements

Gain	Displacement (absolute), μm	Displacement at point 1 (relative)	Displacement (absolute), μm	Displacement at point 2 (relative)
1	414	1	345	1
1/2	234	0.56	176	0.51
1/3	138	0.33	119	0.34
1/4	96	0.23	89	0.26

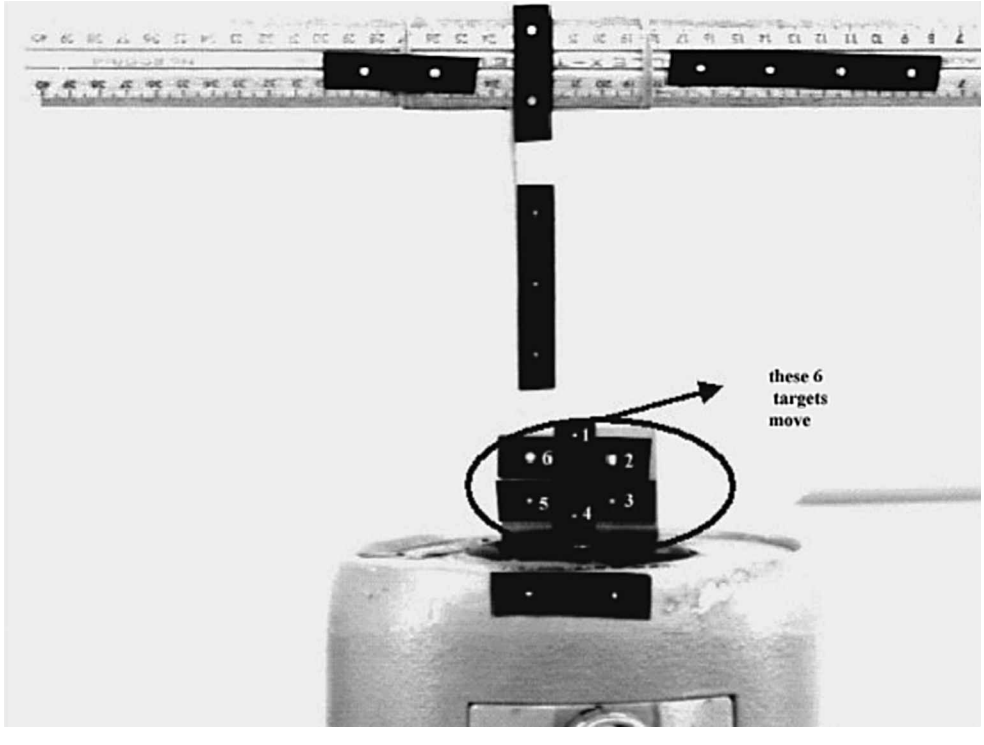

Fig. 5 Target configuration for validation test; targets 1–6 are mounted on a shaker and the remainder are stable.

by the offline photogrammetric approach employing eight camera stations. The distance between targets 2 and 6 is equal to 2.5 cm, this distance being used as the reference scale. For a fixed gain, points 1 and 2 moved through distances that differed by less than the anticipated measurement tolerance, less than 0.05 mm in this case. Also shown in Table 1 are normalized displacements for the two points at each nominal gain, and it can be seen that the estimated relative displacements are equal to (within a very small error) the relative voltage gains driving the shaker.

VI. Experimental Method and Results

As indicated in Fig. 2, the structure to be examined was a wing section held in a supporting frame. Also shown in Fig. 2 is a strobe lamp mounted behind the camera to provide on-axis illumination for the retroreflective targets forming the object point array. Oscillation in the wing structure was induced by the shaker shown in the foreground, and the camera, flash, and shaker were all controlled with reference to a computer-generated sinusoidal wave. As mentioned, adjustments to the time delay between the primary reference signal and the camera ensured that spatial positions within the cycle of oscillation were captured at various phases of motion. The use of only one phase might well have resulted in the capture of motion where the deviation from the mean or static position was very close to zero, thus making the estimate of mode shape unreliable. As a consequence, the time delays used in this experiment were $T = 0, 1/4f$, $2/4f$, and $3/4f$, where f is the frequency of excitation. These delays corresponding to phase shifts of 0, 90, 180, and 270 deg. The selection of four phases both eliminated the problem of minimal deviation and provided a level of redundancy. Static measurements corresponding to absolutely no motion were also performed. This information defined where the targets were positioned in space as distinct from describing the additional differential displacements due to motion. The separation of the displacements into static and dynamic displacements was done outside of the program Australis.

The static displacement corresponds to the shape of the wing section acting under gravity alone and the dynamic shape due to the action of the applied loads. When least squares was used, a monophase mode was extracted from the temporal data on a point-by-point basis. (A monophase mode is a standing wave not a traveling wave.) Using the four equally spaced phase angles guarantees that the monophase mode will be determined with a small variance.

A total of eight different camera positions were used for each photogrammetric survey, and two modes were studied. These modes corresponded to the fundamental bending mode and the torsion mode of vibration, which occurred at 11 and 17 Hz, respectively. As already mentioned, four phases were captured at each frequency. As a result, for each oscillation test there were 8 independent spatial triangulation determinations [using Eq. (4)] and a final 64-image bundle adjustment for the simultaneous determination of all photogrammetric parameters. A notable benefit of the final bundle adjustment is that all *XYZ* object points are explicitly determined in a common reference coordinate system, which is nominally based on the 12 stable targets positioned off the wing (see Fig. 2). As it happened, the exterior orientation parameters did remain very stable over time, and there was, therefore, no significant difference in the *XYZ* coordinates obtained via spatial intersection alone [Eq. (4)] and those computed within the full bundle adjustment [Eq. (2)].

As already mentioned, a standard static measurement of the wing at rest was also carried out via bundle adjustment before each oscillation cycle, though this was not strictly necessary because the same information should also be contained within the positional data obtained for the various phases. Use of the static information, along with the four different phases, enabled a monophase mode to be calculated. The monophase mode is defined as one in which there is no phase change with position except for a possible sign change. This mode can, thus, be represented by using only real numbers or real functions. If the position of the ith target (in the vertical direction) z_i at time t is given by $R_i \cos\theta \cos\omega t + R_i \sin\theta \sin\omega t + \hat{z}_i$, then a least-squares estimation process can be used to determine θ. Although this least-squares problem is nonlinear, an analytical solution can be formulated, though some care needs to be taken in selecting the correct value of θ because multiple solutions are involved. Subsequently, R_i can be determined in a linear manner.

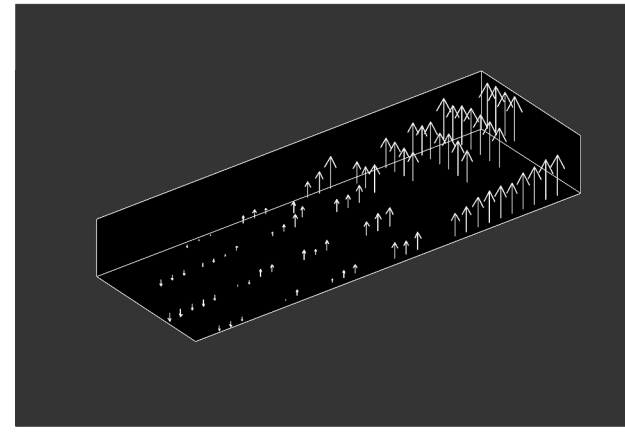

Fig. 6 First mode, fundamental bending.

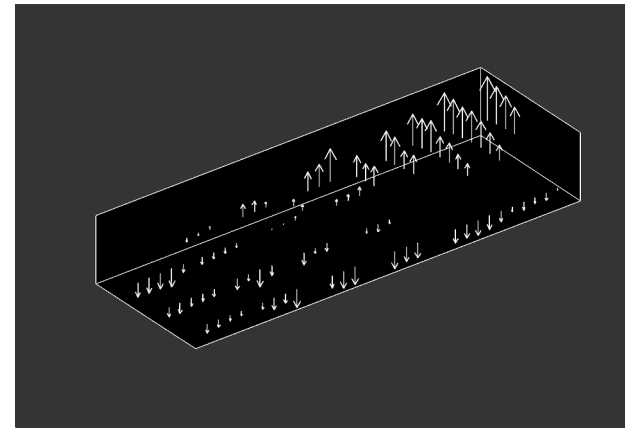

Fig. 7 Second mode, torsion.

Figures 6 and 7 show the final results for the first two modes of vibration of the wing and rig structure. The plot scale of the point displacement vectors $(0, 0, R_i)$ in Figs. 6 and 7 has been exaggerated to better illustrate the pattern of motion. Note that the system is not a pure cantilever because the nodal lines (lines of no motion) running from wing leading edge to wing trailing edge do not occur at the position of attachment of the wing to the rig. Aside from this, the accuracy of determining the modes of vibration was in accordance with design expectations (measurement to 0.05-mm accuracy) and the shape of both modes corresponds to expectations for such a simple structure.

VII. Conclusions

It has been shown that an offline, single-sensor vision metrology approach was successfully employed to determine the dynamic modes of a vibrating structure. Initially a simple experiment (a rigid plate and shaker where the shape of vibration was a priori known) checked the viability of the procedure as well as providing error estimates. A more complex structure involving a wing section was also studied, and in particular its first two modes of vibration were determined, and a discussion of errors was also made. The method used has the advantage of being a low-cost nonintrusive method of determining dynamic responses from structures where the excitation is able to be controlled.

Acknowledgments

The authors would like to thank Michael Konak and Ian Powlesland for the electronics (modifications to the camera), Ken Edmundson for the extensions to the Australis photogrammetric software, Sami Weinberg for providing a component of the real-time software,

and Petra Cox for generating the large amount of software required for the overall system, and for conducting the experiments.

References

[1]Gantmacher, F. R., *Theory of Matrices*, Vol. 1, Chelsea, New York, 1974, Chap. 10, pp. 326–330.

[2]Sokolnikoff, L. S., *Mathematical Theory of Elasticity*, McGraw–Hill, New York, 1956, Chap. 3, pp. 82–91.

[3]Kailath, T., *Linear Systems*, Prentice–Hall, Englewood Cliffs, NJ, 1980, Chap. 2, pp. 31–186.

[4]Dunn, S. A., "Technique for Unique Optimization of Dynamic Finite Element Models," *Journal of Aircraft*, Vol. 36, No. 6, 1999, pp. 919–925.

[5]Slama, C. C. (ed.), *Manual of Photogrammetry*, 4th ed., American Society of Photogrammetry, Falls Church, VA, 1980, Chap. 2, p. 88.

[6]Atkinson, K. B. (ed.), *Close Range Photogrammetry and Machine Vision*, Whittles, Caithness Scotland, U.K., 1996, Chap. 2, p. 33.

[7]Fraser, C. S., "Close Range Photogrammetry and Machine Vision," *Industrial Measurement Applications*, edited by K. B. Atkinson, Whittles, Caithness Scotland, U.K., 1996, pp. 329–361.

[8]Fraser, C. S., "Innovations in Automation for Vision Metrology Systems," *Photogrammetric Record*, Vol. 15, No. 90, 1997, pp. 901–911.

[9]Ganci, G., and Handley, H. B., "Automation in Videogrammetry," *International Archives of Photogrammetry and Remote Sensing*, Vol. 32, No. 5, 1998, pp. 53–58.

[10]Sapp, C. A., "Photogrammetric Assessment of the Hubble Space Telescope Solar Arrays During the Second Servicing Mission," NASA/TP-98-201793, 1998.

[11]Schairer, E. T., and Hand, L. A., "Measurements of Unsteady Aeroelastic Model Deformation by Stereo Photogrammetry," *Journal of Aircraft*, Vol. 36, No. 6, 1999, pp. 1033–1040.

[12]Fraser, C. S., and Edmundson, K. L., "Computational Processes in Digital Close-Range Photogrammetry," *ISPRS International Journal of Photogrammetry and Remote Sensing*, Vol. 55, No. 2, 2000, pp. 94–104.